Environmental Research 218 (2023) 115018

Contents lists available at ScienceDirect

Environmental Research

journal homepage: www.elsevier.com/locate/envres

Post-treatment of matured landfill leachate: Synthesis and evaluation of chitosan biomaterial based derivatives as adsorbents

W.S.M.S.K. Wijerathna [a], L.M.L.K.B. Lindamulla [a,b], K.G.N. Nanayakkara [a,*], R.M.L.D. Rathnayake [a], V. Jegatheesan [b], K.B.S.N. Jinadasa [a]

[a] Department of Civil Engineering, Faculty of Engineering, University of Peradeniya, Peradeniya, 20400, Sri Lanka
[b] School of Engineering and Water: Effective Technologies and Tools (WETT) Research Centre, RMIT University, Melbourne, VIC, 3000, Australia

ARTICLE INFO

Keywords:
Chitosan
Colour
Crosslink
Landfill leachate
Response surface methodology

ABSTRACT

Matured landfill leachate is complex in nature, hence, a single conventional treatment unit is insufficient to remove the contaminants of the leachate to achieve the discharge standards. Furthermore, high levels of organic matter, colour compounds, and iron-based materials form a dark black/brown colour in leachate which is not removed by the biological treatment units. Hence, an Anoxic-Oxic Membrane Bioreactor coupled with a tertiary adsorption unit composed of crosslinked-protonated chitosan was tested for effective removal of the colour of the permeate. Several operational parameters such a pH, contact time, and adsorbent dosage on the adsorptive removal of colour were quantified using sorption-desorption experiments. Furthermore, the biosorbent was characterized using FTIR, SEM, XRD, BET-specific surface area, and pH_{ZPC}. Response Surface analysis confirmed the optimization of operational parameters conducted through traditional batch experiments. Langmuir isotherm model fitted with equilibrium data ($R^2 = 0.979$) indicating a monolayer homogeneous adsorption. Kinetic data followed the Pseudo-Second-Order model ($R^2 = 0.9861$), showing that the adsorbent material has abundant active sites. The percentage removal values show that the colour removal increases with time of contact and dosage of adsorbent, but removal is mainly influenced by the solution pH levels. The experimental results manifested a colour removal efficiency of 96 ± 3.8% obtained at optimum conditions (pH = 2, adsorbent dosage = 20 g/L, contact time = 48 h) along with an adsorption capacity of 123.8 Pt–Co/g suggesting that the studied adsorbent can be used as an environmentally friendly biosorbent in a tertiary unit for colour removal in a treatment system which is used to treat matured landfill leachate.

Funding source

This work was partially supported by the University Research Grant Project (Grant No. URG/2021/19/E) of the University of Peradeniya, Sri Lanka.

1. Introduction

Municipal solid waste (MSW) generation and management have become a serious issue all around the world due to exponential population and social civilization growth, changes in productivity and consumption habits, increasingly affluent lifestyles, unrestricted resource use, and continuous development of the industries and technologies (Foo and Hameed, 2009). With various factors affecting the MSW generation, the per capita MSW generation increases gradually (Costa et al., 2019). These wastes are often dumped at landfills; categorized as open dumps, engineered landfills, and sanitary landfills according to the extent of environmental protection and post-closure plans provided by each landfill type (Vaccari et al., 2019).

Leachate is a toxic, concentrated liquid effluent that is generated from either the rainwater percolation through disposed solid wastes, moisture present in the waste, or the degradation of solid waste disposed of in a landfill. Leachate quality and quantity can be affected by the age of the landfill, seasonal variation of weather, type and composition of waste, factors related to rainfall, groundwater infiltration, and the degree of compaction within the landfill (Luo et al., 2019). Leachate can comprise a wide range of contaminants such as dissolved organic matter, inorganic macro-components, heavy metals, and xenobiotic organic

* Corresponding author.
E-mail addresses: wsmsamanthi94@eng.pdn.ac.lk (W.S.M.S.K. Wijerathna), S3764807@student.rmit.edu.au (L.M.L.K.B. Lindamulla), nadeen@eng.pdn.ac.lk (K.G.N. Nanayakkara), lashithar@eng.pdn.ac.lk (R.M.L.D. Rathnayake), jega.jegatheesan@rmit.edu.au (V. Jegatheesan), shamj@eng.pdn.ac.lk (K.B.S.N. Jinadasa).

https://doi.org/10.1016/j.envres.2022.115018
Received 24 August 2022; Received in revised form 20 November 2022; Accepted 6 December 2022
Available online 7 December 2022

compounds, etc. (Koliyabandara et al., 2020; Ribera-Pi et al., 2021; Vaccari et al., 2019). In Sri Lanka, the leachate is treated as per the guidelines of the National Environmental (Protection and Quality) Regulations imposed by the Central Environmental Authority adhering to the tolerance limits for the discharge of industrial waste into inland surface waters (Wijesekara et al., 2014).

Biological processes, physicochemical processes, membrane filtration processes, advanced oxidative processes, and nature-based systems are some of the techniques which can be used to treat complex wastewater such as landfill leachate, to meet the regulatory discharge standards (Lebron et al., 2021). However, these processes cannot efficiently meet the standards when used as standalone treatment techniques, yet integration of the processes would result in a more efficient treatment system. Biological treatment combined with membrane filtration is a viable solution to treat matured landfill leachate (Bodzek et al., 2006). However, the dark black/brown colour in leachate caused by complex structured natural organic matter, paints, pigments, colour compounds, and iron-based materials are hardly removed by the biological treatment units (Aziz et al., 2011). Our previous studies suggest that (Lindamulla et al., 2022), the Anoxic-Oxic Membrane Bioreactor (A/O MBR) process requires a separate unit which could further assist in the removal of colour from the treated permeate resulting from various interactions among contaminants and minerals, which is not removed by the biological processes.

Adsorption, which is a physicochemical treatment, is a widely used post-treatment polishing technique for contaminant removal. For instance, Azis et al. (2021) evaluated a sand filtration-activated carbon adsorption system to remove the fungicide content of a biologically treated effluent while Hagemann et al. (2020) used wood-based activated biochar for organic micropollutant removal. Furthermore, studies by Chaouki et al. (2017), De et al. (2019), Fenyvesi et al. (2020), and Thongkrua and Suriya (2022) have verified the use of adsorption as a viable post-treatment technique that can be used for efficient contaminant removal from the biologically treated wastewater flows. In addition, the use of adsorption for colour removal has been studied because of its high performance, economic feasibility, and simplicity (Zafar et al., 2020). Activated carbon has been employed as the most common adsorbent for the removal of organic substances as well as for the removal of colour due to its favourable characteristics such as; high surface area, microporous structure, and high adsorption capacity (San-Pedro et al., 2020). However, the commercial cost and the expensive regeneration process are several disadvantages associated with the use of activated carbon as the adsorbent material. Therefore, much research is being conducted on developing low-cost adsorbents that can be used for wastewater treatment. A few examples of cost-effective adsorbents include; zeolite (Aziz et al., 2020), limestone composites (Aziz et al., 2011; Foul et al., 2009; Rosli et al., 2018), peat composites (Rosli et al., 2017), oat hull (Ferraz and Yuan, 2020), sugarcane bagasse (Azmi et al., 2014), tamarind fruit seed (Foo et al., 2013a), etc.

It has been reported that the use of biosorbents has several advantages such as ease of production and lower costs as compared to activated carbon (Nassar and El-Geundi, 1991). Chitin, being the second most abundant natural polymer in the world, forms chitosan after deacetylation (Alves et al., 2021). Chitosan has proven to be a prominent adsorbent due to its abundance in the environment, enhanced adsorption capacity arising from the higher surface area, and efficient contaminant removal by the amine and hydroxyl functional groups present in the chemical structure (Rupasinghe et al., 2022; Vieira et al., 2011). However, chitosan needs to be stabilized with a suitable crosslinking agent for it to be used effectively at low pH conditions, otherwise, it dissolves and loses the ability to bind adsorbate (Filipkowska et al., 2014). Among various alternatives, glutaraldehyde has been identified as a promising option because of its ease of processing, lower cost, and effective crosslinking capacity (Mahaninia and Wilson, 2017). Furthermore, it allows crosslinking of aldehyde groups prevalent in glutaraldehyde promoting stability in a wide range of pH and higher adsorptive capacity (Nagireddi et al., 2017).

Chitosan, in its various forms; films, beads, nanoparticles, etc. have been used to remove the colour from wastewater. Shajahana et al. (2017) studied the fungal chitosan nanoparticles synthesized using *Cunninghamella echinulata* (Thaxter) to investigate its adsorption behaviour towards remazol brilliant blue, methyl orange, disperse red 13, napthol blue-black, and Chicago sky blue 6B where they observed Chicago Sky blue had the highest affinity towards chitosan nanoparticles. Vedula and Yadav (2022) developed a chitosan lignin membrane for methylene blue removal while Tahari et al. (2022) and Hussain et al. (2021) experimented with chitosan/tannin/montmorillonite film and chitosan-coated sodium zeolite composite film respectively, for methyl orange removal. Copper nanoparticle-impregnated chitosan biocomposite was used by Shukla et al. (2021) for crystal violet removal whilst Mohd Halim et al. (2022) investigated the efficiency of chitosan when used for making composite electrodes along with graphite and polyvinyl chloride. Crosslinked chitosan tripolyphosphate beads prepared by Sánchez-Duarte et al. (2012) and crosslinked succinyl chitosan beads prepared by Huang et al. (2011) have shown considerable removal efficiencies towards Allura red food dye and methylene blue respectively.

Though chitosan is a well-researched adsorbent and a coagulant for contaminant removal, after an extensive literature review, it was observed that there is only a very limited number of research carried out concerning its application as a tertiary treatment unit of a landfill leachate treatment system, especially focusing on colour removal. In addition, almost all the previous studies have considered colour removal using synthetic dyes, instead of considering the complexity of real wastewater flows. Hence, it was identified that further investigations are required to understand the behaviour of chitosan in treatment systems for contaminant removal under practical situations. In addition, the kinetics and mechanisms of the adsorption process need more insight due to the selectivity and complexity of the system when applied in practical schemes.

Furthermore, Response Surface Methodology (RSM) provides reliable information to optimize the experimental process ultimately providing an empirical model that can be used to fit the experimental data, saving a significant portion of time compared to the traditional batch experiment approach. The method itself is less laborious and can be used to study the interactions among several factors with a limited number of experimental runs (Adeleke et al., 2017; Ghani et al., 2017; Ravikumar et al., 2007).

Hence, the study aimed to develop a polishing treatment unit for an Anoxic-Oxic Membrane Bioreactor (A/O MBR) system which is used for landfill leachate treatment (Fig. S1) to treat the effluent up to the discharge standards in terms of colour. In that context, objectives were defined as (i) to develop and characterize the adsorbents derived from chitosan to post-treat mature landfill leachate (ii) to investigate the adsorption efficiency of modified biosorbents in colour removal using traditional linear optimization batch experiments while studying the regeneration capacity of the adsorbent and (iii) to study the colour removal process through RSM using factorial design approach.

2. Materials and methods

2.1. Materials

2.1.1. Preparation of crosslinked protonated chitosan beads

Chitosan powder was obtained from the Norwegian University of Life Sciences as the raw material and the physical modification was done using glacial CH_3COOH and NaOH following a general procedure (Ngah and Fatinathan, 2008; Rupasinghe et al., 2022). Briefly, 3 g of chitosan powder was dissolved in 1% of CH_3COOH and stirred using a magnetic stirrer for 3 h at room temperature. Chitosan beads (CHT) were prepared by adding the solution dropwise to 1M NaOH solution using a syringe, at

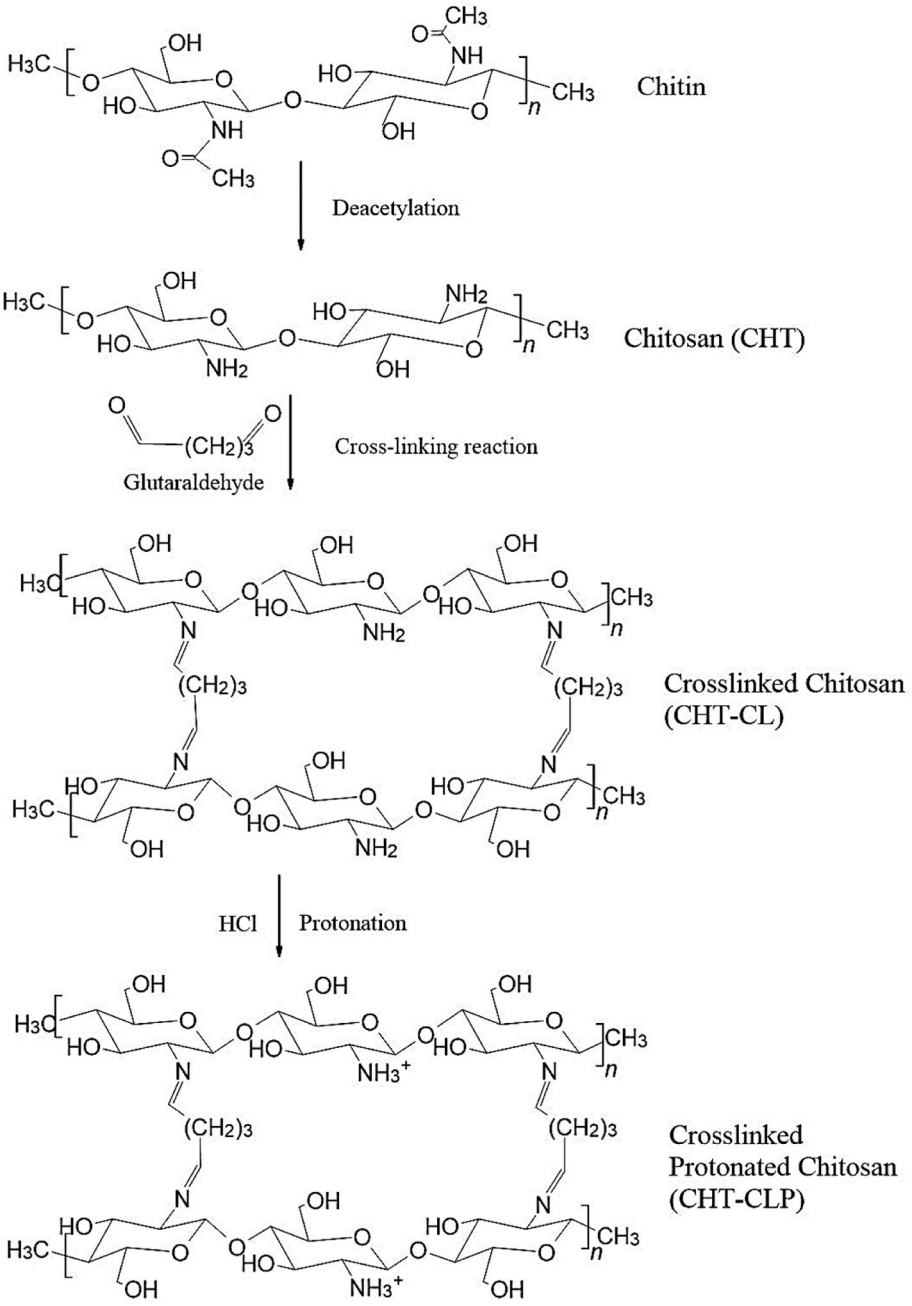

Fig. 1. Modification process of crosslinked protonated chitosan (CHT-CLP).

constant pressure and the material was kept in NaOH for 24 h. After a thorough washing of CHT with distilled water to remove excess NaOH, chemical modification to the chitosan beads was done by crosslinking using Glutaraldehyde solution (Grade II, 25% in H_2O). The wet beads were crosslinked with 2.5 wt % glutaraldehyde solution (Glutaraldehyde solution: Wet chitosan beads = 10 ml: 1 g) and the mixture was kept at 20 °C in the Lovibond Thermostatic Cabinet for 48 h. Excess glutaraldehyde in the crosslinked chitosan material (CHT-CL) was washed using distilled water and thereafter, protonation of beads was done by soaking the beads in concentrated HCl for 30 min. The functional group development during the modification process is described in Fig. 1. Finally, resulting protonated crosslinked chitosan beads (CHT-CLP) were washed with distilled water at a constant pH and dried at 34 °C, and stored in the desiccator until further use. All the chemicals and the reagents used were of analytical grade.

2.1.2. Characterization of raw and modified adsorbents

X-ray Diffraction (XRD) analysis for the materials was carried out to identify the change in the crystalline structures and the mineral composition of CHT, CHT-CL, CHT-CLP. The XRD spectra for all materials were obtained in the 2θ range from 5° to 80° using an X-ray Diffractometer (Bruker D8 Advanced Eco Powder XRD, USA). To identify the change in surface morphology and microstructure, Scanning Electron Microscopy (SEM) images were taken at high and low magnification levels using Scanning Electron Microscopy (Carl Zeiss EVO LS 15 SEM, Germany). The functional groups in CHT, CHT-CL, CHT-CLP were identified by analysing the peak frequencies in Fourier Transform Infrared (FTIR) spectra (PerkinElmer Spectrum Two™, USA). Specific surface area (SSA) increase from CHT-CL to CHT-CLP due to modifications, was determined using the Brunauer-Emmet-Teller (BET) method by N_2 adsorption at 77.35 K using Autosorb iQ Surface Area Analyzer (Quantachrome® AsiQwin™, Austria). The surface area was reported

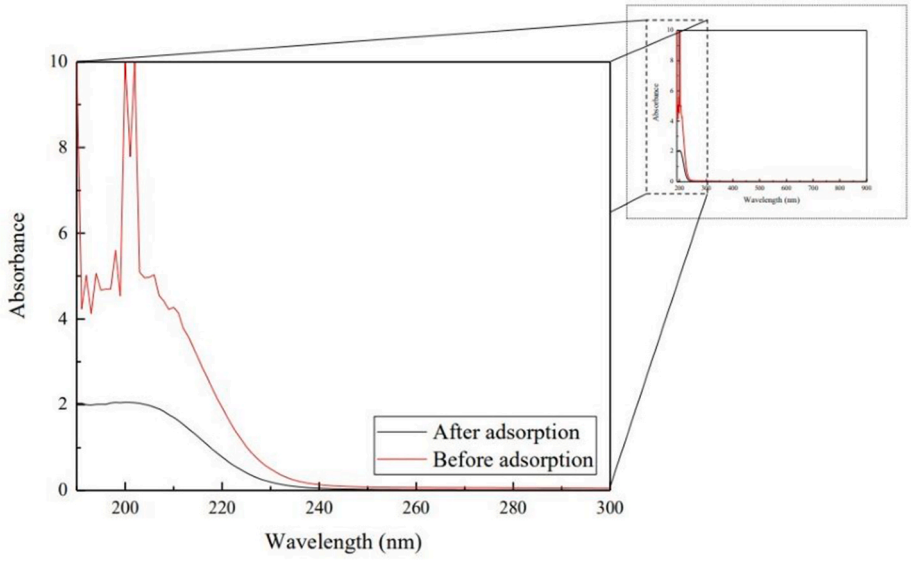

Fig. 2. UV–Visible Spectrum of A/O MBR permeate before and after CHT-CLP adsorption.

using the Multi-Point BET method whereas the pore volume and the pore radius were reported using the Barret Joyner Halenda (BJH) method analysed by the same instrument. The pH value at which the net surface charge of the material is null in the aqueous media (pHzpc) was determined using the salt addition method following the method described in Bakatula et al. (2018).

2.1.3. Characterization of A/O MBR permeate

The permeate before and after the adsorption was diluted 100 times and scanned by a UV–Visible spectrophotometer (UV-2600/2700 - Shimadzu, Japan) to understand the degradation of aromatic compounds and other organic matter. Furthermore, other wastewater quality parameters such as BOD_5, COD, and nutrients were analysed in the samples using standard methods (APHA, 2002) and the heavy metal concentrations of the solutions were measured using Atomic Adsorption Spectrophotometer (AA-7000 – Shimadzu, Japan).

2.2. Adsorption experiments

2.2.1. Batch experiments

Permeate was collected from the outlet of A/O MBR treating the landfill leachate from the Gohagoda Landfill site, Kandy, Sri Lanka. Batch experiments were conducted to investigate the effect of different influential parameters such as pH, contact time, and adsorbent dosage. The initial colour concentration of permeate was maintained at 3200 ± 200 Pt–Co. Samples were placed in the shaking incubator (Thomas AT12R Thermostatic, Japan) at 200 rpm for homogenous shaking for all experiments and all experimental studies were conducted by fixing the temperature of the incubator at 25 °C. The supernatant was filtered with 0.45 μm PES filter paper and the filtrate was analysed for colour using the portable colorimeter (Hach DR 900, USA).

2.2.2. Regeneration studies

Regeneration studies of CHT-CLP were conducted using 1M NaOH, 1M HCl and distilled water to study the efficiency and the reusable capacity of the CHT-CLP. CHT-CLP which was used under the optimum adsorption conditions was regenerated using the eluting agents by shaking at 200 rpm for 24 h. Thereafter, the adsorbent was thoroughly washed with distilled water to remove excess acid/base and then again tested under optimum conditions. Three consecutive runs with these conditions were investigated to observe the decrease in the adsorption capacity of CHT-CLP.

2.3. Design of experiments and RSM analysis

RSM was used to study the effects of three independent variables (pH, Adsorbent dosage, and contact time) on the removal of colour. The Central Composite Design (CCD) method was used to determine the number of experiments needed as trial runs for the optimization of the variables as well as responses. As the input variable ranges to create the trial runs in CCD, the pH ranged from 2 to 11, the adsorbent dosage ranged between 0.5 and 30 g/L whereas the contact time varied between 0 and 54 h. The Design Expert 13 software was used to analyse the experimental results and to investigate the responses of the model. The significance of the variables in the adsorption process was analysed using the analysis of variance (ANOVA) and the adjusted coefficient of determination (R^2 adj) was used to check the Lack of Fit of the model.

3. Results and discussion

3.1. Permeate and adsorbent characterization

3.1.1. Permeate characterization

Fig. 2 shows the UV–Visible absorption spectra of the A/O MBR permeate before and after adsorption treatment using CHT-CLP. When considering the 190–900 nm wavelength range, there was no apparent peak in the spectrum of permeate. The inability to observe significant peaks in the UV–Visible spectrum of permeate could be attributed to the complexity of the organic matter present in landfill leachate, and hence in treated permeate (Jiang et al., 2022). The peaks in the <210 nm range could be arising from chromophores such as alkyne, carbonyl, carboxyl, methylamine, benzene, toluene, and phenol groups which may present in the permeate (Pratiwi and Nandiyanto, 2022). A significant decrease in the intensity of bands was observed after adsorption. This could have been caused due to molecular weight and aromaticity reduction of the organic matter as a result of adsorption by CHT-CLP (Castillo-Suárez et al., 2018).

The A/O MBR effluent samples were analysed for BOD_5, COD, PO_4^{3-}, NO_3^-, NO_2^- and SO_4^{2-} and the values were obtained as 258 mg/L, 650 mg/L, 86 mg/L, 206 mg/L, 0 mg/L and 242 mg/L, respectively. In addition, Zn(II) and Pb(II) were analysed for heavy metal content and obtained values of 1.056 mg/L and 0.012 mg/L, respectively, which were below the tolerance limit values. Though BOD_5 and COD values exceeded the specified standards for discharge (30 mg/L and 250 mg/L, max respectively), environmental guidelines have not provided values

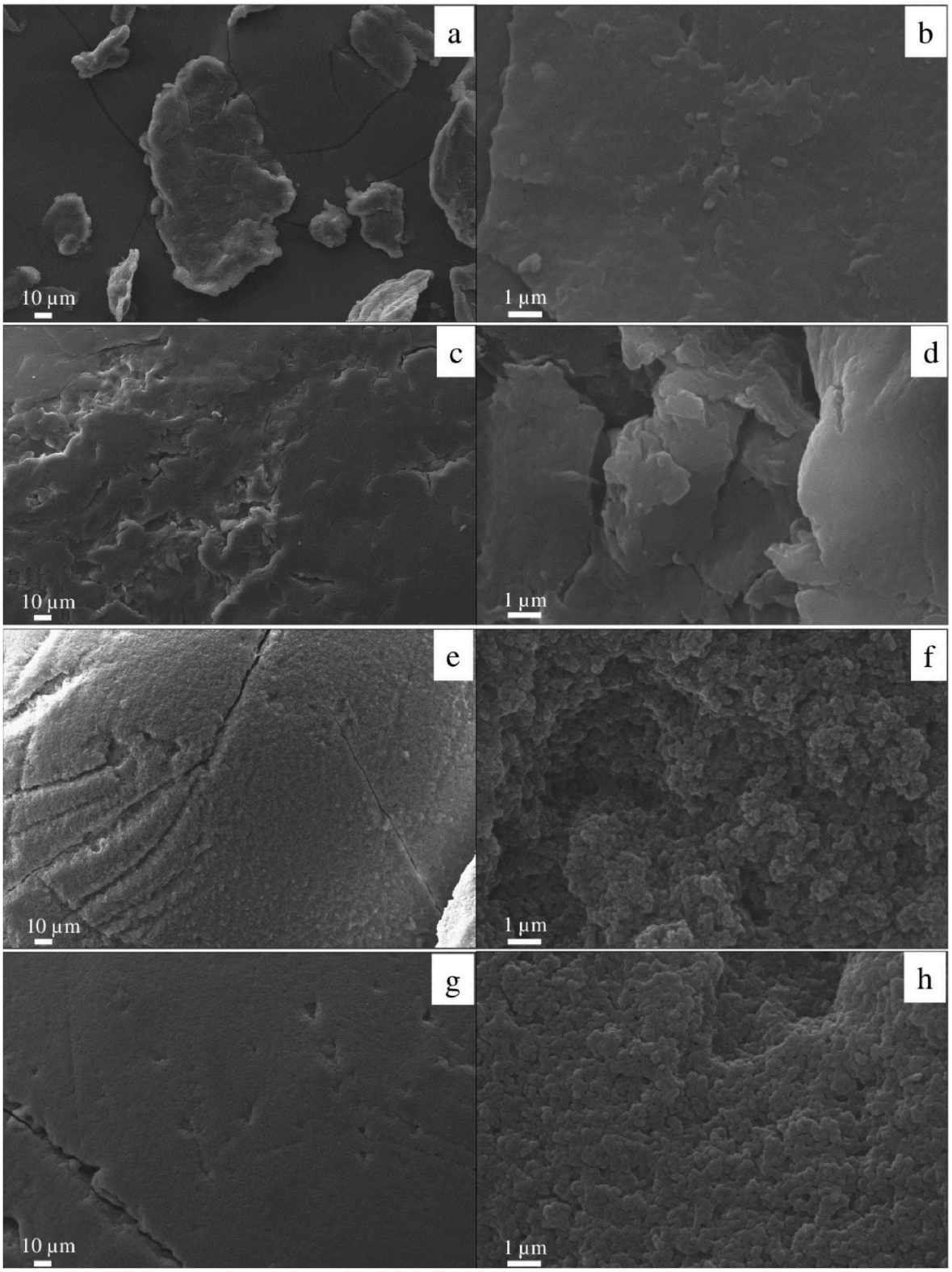

Fig. 3. SEM images of (a) raw chitosan powder – 1000 X, (b) raw chitosan powder – 20.00 K X, (c) chitosan beads – 1000 X, (d) chitosan beads – 20.00 K X, (e) Cross-linked chitosan – 1000 X, (f) Cross-linked chitosan – 20.00 K X, (g) Cross-linked protonated chitosan – 1000 X, (h) Cross-linked protonated chitosan – 20.00 K X.

for nutrient removal standards (CEA, 2008). Nevertheless, the organic and anion content in the permeate proved that they might be the cause of the colour in the permeate. Hence, the study was limited to the removal of colour-causing organic and anionic content from the permeate based on colour removal.

3.1.2. Adsorbent characterization

The peaks at 12° and 20° in the XRD pattern of chitosan were attributed to the natural peaks observed in raw chitosan material [Fig. S2]. The peak at 12° disappeared after modifying with glutaraldehyde and the peak at 20° weakened after the protonation stage,

Table 1
Specific surface area and pore volume of adsorbents.

Adsorbent	BET Specific Surface Area (m^2/g)	Pore Volume (cm^3/g)	Reference
CHT-CL	38.42	0.04	Present Study
CHT-CLP	45.80	0.05	
CHT-CL	121.6	0.36	Suguna et al. (2011)
CHT-CL	1.45	N/A	Ngah et al. (2005)
CHT-CL	0.52	N/A	Ngah and Fatinathan (2008)
CHT-CL	0.171	N/A	Bui et al. (2020)
CHT-CL	0.37	N/A	Jawad et al. (2019)

indicating the weakening of hydrogen bonds between the molecules during the modification. The crystalline nature of the material, which prevented the amine groups from binding efficiently with the adsorbate, has converted to a more amorphous nature, making $-NH_3^+$ sites more accessible. Therefore, the contamination adsorption can also increase in the CHT-CLP structure (Huang et al., 2012; Igberase et al., 2017).

SEM images of the material before and after each modification step [Fig. 3] and after the adsorption experiments [Fig. S3] were obtained at low and high magnification levels to examine the surface morphology changes. Crosslinked and protonated crosslinked chitosan materials showed the development of surface roughness, thereby increasing the contact area to facilitate pore diffusion during adsorption (Suguna et al., 2011). In addition, it can be observed that the irregularities in the raw material are removed and the modified material has a uniform distribution of features [Fig. 3]. SEM images obtained after adsorption experiments showed that the pores have been filled due to the adsorption of contaminants which reasons out the high adsorption capacity.

The FTIR spectrum of the raw chitosan showed peaks corresponding to the functionalities present in the structure [Fig. S4]. The sharp peak observed at 1634 cm^{-1} was attributed to $-NH_2$ bending vibration and the shift in peak at 1577 cm^{-1} confirmed the presence of NH_3^+ groups in CHT-CLP formed in the modification process (Huang et al., 2012). The peak at 1382 cm^{-1} was assigned to the $-CH_3$ symmetrical deformation mode in the amide group and 1027 cm^{-1} is the skeletal stretching vibrations of C–O which is a characteristic peak of polysaccharide structure in chitosan (Sivakami et al., 2013). However, the peak at 1577 cm^{-1} shifted to lower wavenumbers showing the electrostatic attraction between negatively charged colour-causing contaminants and positively charged NH_3^+. The broad band of CHT-CLP at 3285 cm^{-1} indicated the presence of exchangeable protons which could be from amine and alcohol groups (Igberase et al., 2017). After adsorption, the intensity of the peaks reduced considerably indicating the complexation and bonding between contaminants and the functional groups in the CHT-CLP (Huang et al., 2012; Liu et al., 2016).

Specific surface area (SSA) and pore volumes obtained from the BET analysis are shown in Table 1. SSA values reported by Suguna et al. (2011) amount to more than thrice of values observed in this study for CHT-CL. However, comparatively, higher SSA was obtained for CHT-CL than the reported values in Ngah et al. (2005) and Ngah and Fatinathan (2008). Furthermore, an additional 19.2% increase in SSA was observed after modifying CHT-CL into CHT-CLP and a similar increase of around 25% was observed for the pore volume as well. The increase in SSA results in an enhancement in the adsorption sites facilitating efficient colour removal by CHT-CLP. However, though there is an increase in the surface area due to irregularities in the surface as observed in the SEM images, the low porosity values presented in Table 1 may be due to the compacted chemical structure caused by crosslinking of chitosan and blockage of internal pores of chitosan by glutaraldehyde molecules (Vakili et al., 2019).

The pH_{ZPC} gives the pH value at which the surface charge components become null and this could be used as an indicator to effectively select the adsorbents suitable for specific contaminant removal. The pH_{ZPC} of CHT-CLP was found to be around 4.8 [Fig. S5] indicating an acidic nature of the surface of the material. Hence, at pH < 4.8 conditions, CHT-CLP effectively removes anions and at pH > 4.8 the adsorbent effectively removes cations via electrostatic attraction (Guibal et al., 1998).

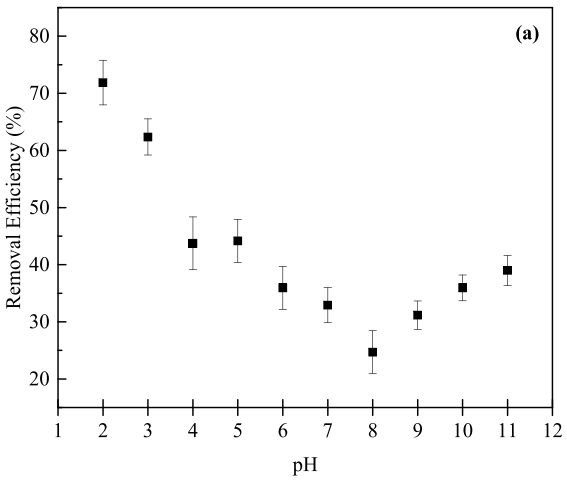

[Contact time = 24 Hrs; Adsorbent dosage = 10 g/L; Rotating speed = 200 rpm]

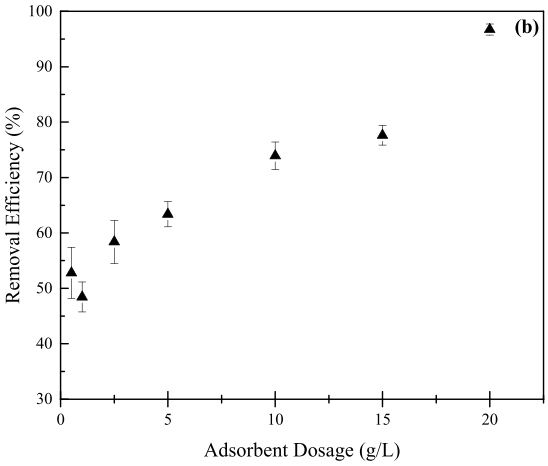

[Contact time = 24 Hrs; pH = 2; Rotating speed = 200 rpm]

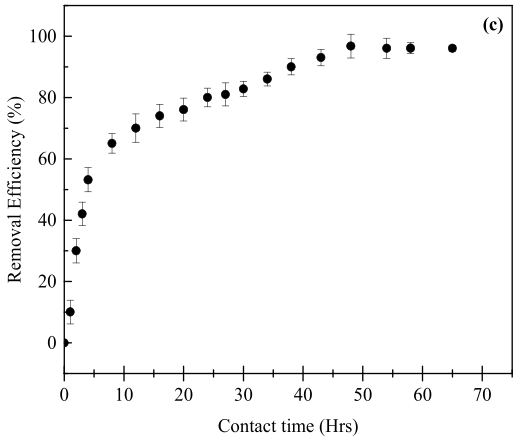

[pH = 2; Adsorbent dosage = 20 g/L; Rotating speed = 200 rpm]

Fig. 4. Colour removal efficiency by CHT-CLP as a function of (a) pH, (b) adsorbent dosage and (c) contact time.

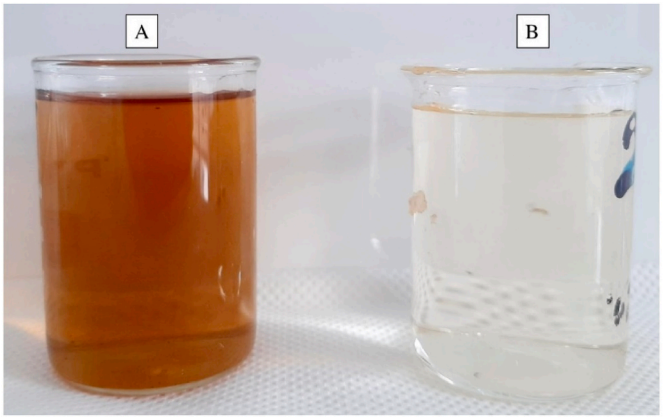

Fig. 5. A/O MBR permeate (A) before and (B) after adsorption.

3.2. Adsorption batch studies

The pH of the solution significantly controls the adsorption efficiency. Variation of colour removal with pH is shown in Fig. 4 (a). The highest colour removal was observed at pH = 2 with 72 ± 3.9% removal and the lowest at pH = 7 with 25 ± 3.1% removal, hence the subsequent experiments were conducted at pH = 2 conditions. These observations are in agreement with studies done by Aziz et al. (2010). The higher colour removal at low pH values indicated that the colour could have been mainly caused by negatively charged ions present in the leachate which are removed by the positively charged $-NH_3^+$ functional groups which impart a cationic character enabling strong electrostatic interactions (Filipkowska et al., 2014; Narayana, 2022). Furthermore, at low pH values, the charge density of CHT-CLP increases while reducing the polar nature of natural organic matter substances leading to an improved removal efficiency (Vogelsang et al., 2004). In addition, at low pH values $-NH_3^+$ creates an electronic repulsion between metal ions. When the pH value is increased, the amino groups free from protonation and hence the hydrogen ion concentration reduces thus reducing the colour causing anion uptake (Sun et al., 2006). This observation agrees with the discussion on pH_{ZPC} as well. However, a further increase in the pH above 8 has enhanced the colour removal slightly. At higher pH values the metal ions present in the leachate can be precipitated as chlorides or hydroxides, reducing the colour of the permeate (Suguna et al., 2011).

The adsorbent dosage is an important parameter in the determination of the adsorption capacity of an adsorbent at given conditions. As shown in Fig. 4 (b) colour removal was enhanced with the increase in the adsorbent dosage due to obvious reasons such as the increase in the number of active sites. Since 95 ± 1.0% colour removal was obtained, further increase in the dosage was not considered for tests and 20 g/L dosage was considered as the optimum dosage.

When considering colour removal as a function of contact time (Fig. 4 (c)), the colour removal increased sharply up to 24 h and then the removal efficiency reached 96 ± 3.8% after 48 h. Thereafter, though the removal efficiency remained almost constant, the adsorption capacity decreased with increasing dosage which could be the effect of unsaturated adsorption sites (Ngah and Fatinathan, 2008).

It is plausible to suggest that at the beginning of the experiment, the concentration gradient between the fluid film and the available adsorbent pore sites was high, hence the colour removal rate was high. Subsequently, the adsorption rate decreased which could be due to the saturation of functional groups with contaminants and slow pore diffusion of the solutes into the adsorbent (Huang et al., 2012). These observations along with SEM images supported a few of the mechanisms of adsorption as to the chemical binding of contaminants to adsorption sites, the diffusion through the fluid film around the CHT-CLP bead and diffusion through the pores to the internal adsorption sites. Ultimately, 20 g/L and 48 h were concluded as the optimum dosage and contact time, respectively. Fig. 5 shows the colour removal performed by CHT-CLP under the identified optimum conditions.

Table 2 exhibits a comparison of adsorption capacities in various adsorbents studied in the literature. Considering the removal efficiency, CHT-CLP has shown the highest removal percentage in terms of colour in similar studies. Furthermore, comparatively, the adsorbent proposed in this study; CHT-CLP has shown a significantly high adsorption capacity than the studies conducted by Thongkrua and Suriya (2022) and Abuabdou et al. (2019). However, palm bark powder used by Chaouki et al. (2021) has shown an adsorption capacity of nearly twice that of CHT-CLP whilst tamarind fruit seed-derived carbon experimented by Foo et al. (2013b) has shown around 36% high adsorption capacity with respect to CHT-CLP. Considering the modifications done to the adsorbent, these differences could have been caused by the protonation effect of the adsorbent by which the colour-causing contaminants present in leachate, mainly negatively charged ions, are removed by CHT-CLP. Nevertheless, all these studies prove that the use of adsorption as a post-treatment for biologically treated landfill leachate is an effective treatment scheme which could be adopted in treating the landfill

Table 2
Adsorption capacities and removal efficiencies of various adsorbents on colour removal from landfill leachate.

Wastewater condition	Adsorbent	Removal Efficiency (%)	Adsorption capacity	Optimum removal conditions					Reference
				pH	Contact time (h)	Adsorbent dosage (g/L)	Temperature (°C)	Rotating speed (rpm)	
Biologically treated landfill leachate	Organosorb 10 MB (manufactured by Chemipol)	45	–	–	5	20	20	–	(Castrillón et al., 2010; Marañón et al., 2009)
Coagulation-flocculation pre-treated landfill leachate	Palm bark powder	59	255 mg/g	5.6	3	9	25	–	Chaouki et al. (2021)
Semi-aerobic landfill leachate	Tamarind fruit seed-derived activated carbon	91.23	168.57 Pt–Co/g	6	2.67	0.030	30	–	Foo et al. (2013b)
Raw landfill leachate	KOH-activated palm oil fuel ash	85.37	28.329 Pt–Co/g	–	3	100	–	250	Abuabdou et al. (2019)
Biologically pre-treated landfill leachate	Corn cob-derived $ZnCl_2$-impregnated activated carbon	88.6 ± 0.2	10.3 ± 0.02 mg/g	10	0.67	12	30	120	Thongkrua and Suriya (2022)
Biologically pre-treated landfill leachate	Crosslinked-Protonated Chitosan	96 ± 3.8	123.8 Pt–Co/g	2	48	20	25	200	Present Study

Table 3
Results for kinetic models.

Model	Linear form of the equation	Parameters	
Pseudo First Order	$log\,(q_e - q_t) = log\,q_e - \frac{k_1 t}{2.303}$	R^2	0.8372
		k_1	0.01082
		$q_{theoritical}$	208.6
Pseudo Second Order	$\frac{t}{q_t} = \frac{1}{k_2 q_e^2} - \frac{1}{q_e} t$	R^2	0.9861
		k_2	0.00068
		$q_{theoritical}$	126.6
Intra-Particle Diffusion	$q_t = k_i t^{0.5} - \alpha$	R^2	0.9268
		k_i	15.727
		α	16.923
Elovich	$q_t = \frac{1}{b} ln(ab) + \frac{1}{b} ln(t)$	R^2	0.9732
		a	103.73
		b	0.0365

q_t (Pt–Co g^{-1}): Amount of adsorbate per unit mass of adsorbent at time t
q_e (Pt–Co g^{-1}): Amount of adsorbate per unit mass of adsorbent at equilibrium state
k_1 (h^{-1}): Equilibrium rate constant of PFO
k_2 (g Pt–Co^{-1} h^{-1}): Equilibrium rate constant of PSO
k_i (Pt–Co g^{-1} $h^{-0.5}$): Intra-particle diffusion rate constant
α (Pt–Co g^{-1}): Constant which relates to the thickness of the boundary layer
a (Pt–Co g^{-1} h^{-1}): Initial adsorption rate constant of the Elovich model
b (g Pt–Co^{-1}): Desorption rate constant of the Elovich model

Table 4
Results for isotherm models.

Model	Equation		Parameters	
Langmuir	Linear form	$\frac{1}{q_e} = \frac{1}{q_m} + \frac{1}{q_m k_a} \frac{1}{C_e}$	R^2	0.979
			q_m	1666.7
			k_a	0.0043
	Nonlinear form	$q_e = q_m \frac{k_a C_e}{1 + k_a C_e}$	R^2	0.63105
			q_m	2.08E7
			k_a	2.95E-8
Freundlich	Linear form	$log\,q_e = log\,k_f + \frac{log\,C_e}{n}$	R^2	0.512
			k_f	1.842
			n	1.191
	Nonlinear form	$q_e = k_F\, C_e^{1/n}$	R^2	0.97718
			k_f	2.49E-8
			n	0.2984
Dubinin-Radushkevich	Linear form	$ln\,q_e = ln\,q_m - B_{DR}\varepsilon^2$	R^2	0.7475
		$\varepsilon = RT\,ln\left[1 + \frac{1}{C_e}\right]$	q_m	2631.74
			B_{DR}	0.2573
	Nonlinear form	$q_e = q_m\, exp^{(-B_{DR}\,\varepsilon^2)}$	R^2	0.94468
		$\varepsilon = RT\,ln\left[1 + \frac{1}{C_e}\right]$	q_m	5522.14
			B_{DR}	0.5731
Temkin	Linear form	$q_e = B\,ln\,A_T + B\,ln\,C_e$	R^2	0.2379
			A_T	0.0068
		$B = \frac{RT}{b_T}$	B	560.03
			b_T	4.424

C_e (Pt–Co l^{-1}): Equilibrium colour concentration in solution
q_e (Pt–Co g^{-1}): Colour concentration in the adsorbent
q_m (Pt–Co g^{-1}): Maximum monolayer adsorption capacity of the adsorbent
k_a: Langmuir equilibrium sorption constant related to adsorption energy
k_f: Measure of adsorption capacity
n: Measure of the degree of favourability of the adsorption
B (J mol^{-1}): Related to the heat of sorption
A_T (l g^{-1}): Temkin isotherm equilibrium binding constant
b_T: Dimensionless Temkin isotherm constant
R: Universal gas constant (8.314 J/mol K)
T: Temperature at 298 K
B_{DR} (mol^2 J^{-2}): Dubinin-Radushkevich isotherm constant
ε: Dimensionless Dubinin-Radushkevich isotherm constant

leachate up to the discharge standards.

3.3. Sorption kinetic and isotherm studies

Pseudo First Order, Pseudo Second Order, Intra-Particle Diffusion and Elovich models were used to study the kinetic behaviour of the adsorption process. As shown in Table 3, data were well fitted to the Pseudo Second Order kinetic model based on a high R^2 value of 0.9861. In addition, the $q_{theoritical}$ values calculated are considered to be in reasonable agreement with $q_{experimental}$ values. These results suggested that chemical adsorption might be involved in the adsorption process. In addition, the Elovich model also showed a considerably higher R^2 value (0.9732) indicating that the real media surface could be heterogeneous based on their energy (Wang and Guo, 2020a).

Langmuir, Freundlich, Dubinin-Radushkevich and Temkin isotherm models were used to describe the adsorption characteristics of the adsorbent. In this study, equilibrium experimental data were fitted to both linear and nonlinear forms of a few isotherm models. As per Table 4, the equilibrium data fitted well with the linear Langmuir model with the highest R^2 value of 0.979, indicating that the system adheres to monolayer adsorption and a homogeneous distribution of adsorption sites of CHT-CLP. Furthermore, in Langmuir isotherm, it is assumed that every adsorption site and the binding ability of the adsorbate are equivalent and independent of whether the adjacent sites are occupied or not. Therefore, in this system, the adsorption energy can be confirmed as constant, equally distributed over the entire adsorbent surface and the interactions between the adsorbate molecules are negligible (Wang and Guo, 2020b). Hence, the adsorption mechanism can be strongly suggested as the formation of uniform adsorption of adsorbate, resulting in a monolayer coverage on the adsorbent (Choi et al., 2020).

A dimensionless constant known as the separation factor R_L [$R_L = {}^1/_{1 + k_a C_i}$; where k_a (L/Pt–Co) refers to the Langmuir constant and the C_i denotes the adsorbate initial concentration (Pt–Co/L)] was calculated from the results obtained for the Langmuir isotherm model to check the favourability of the adsorption (Sowmya and Meenakshi, 2014). R_L value was obtained as 0.0677 indicating a favourable nature ($0 < R_L < 1$) of CHT-CLP towards colour removal (Foo and Hameed, 2010).

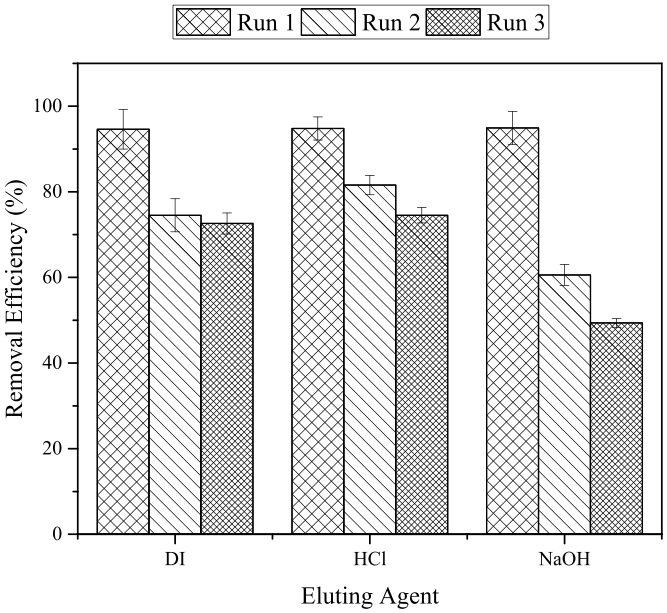

Fig. 6. Regeneration Capacity of CHT-CLP (pH = 2; contact time = 48 h; adsorbent dosage = 20 g/L; rotating speed = 200 rpm).

3.4. Regeneration of CHT-CLP

The reusability of adsorbent is an important aspect of adsorption studies from an environmental and economic point of view. Hence, in this study, 1M NaOH, 1M HCl and distilled water were used as eluting agents for recovering the material. Amongst them, HCl proved a regenerated capacity of 78.6% after the 3rd run and surprisingly distilled water also recovered the material to a near-high capacity as HCl (76.7%) even after a 3rd cycle of material reuse (Fig. 6), indicating the feasibility of recovering the adsorbent. Huang et al. (2012) have reported similar

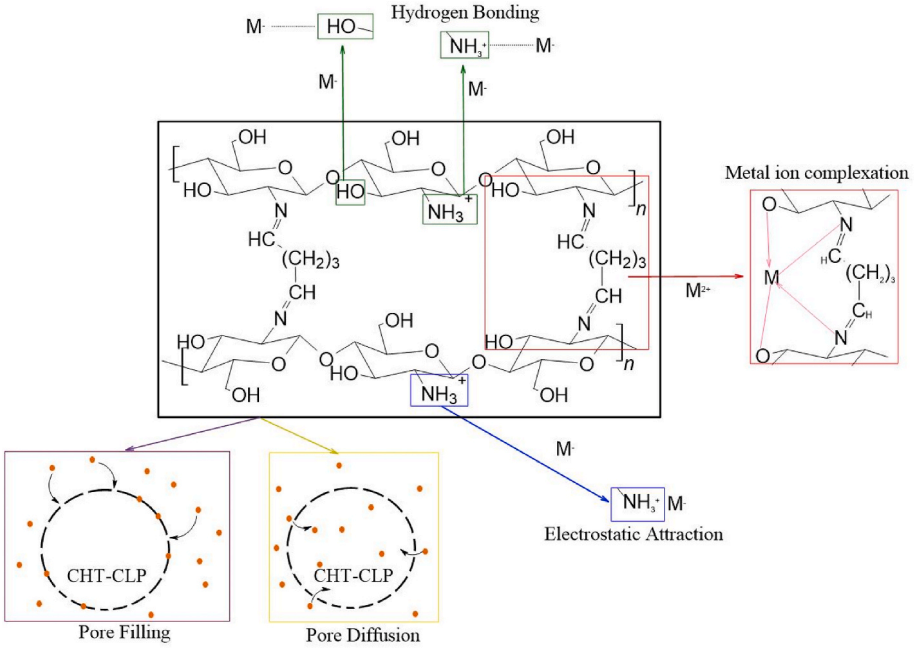

Fig. 7. Proposed adsorption mechanisms of CHT-CLP in removing colour causing contaminants. (For interpretation of the references to colour in this figure legend, the reader is referred to the Web version of this article.)

observations for recovering glutaraldehyde crosslinked protonated chitosan membranes in fluoride removal using acidic eluting agents. Nevertheless, an overall decrease in the adsorption capacity might have been partly caused due to the slight loss of the adsorbent mass during the regeneration process (Tabrizi and Yavari, 2020) and might also be associated with incomplete desorption and strong complexes made between the adsorption sites and metal ions causing a decline in effective adsorption sites (Vakili et al., 2018).

3.5. Proposed adsorption mechanisms of contaminant removal

The adsorption mechanism is complex as illustrated in Fig. 7. The co-existence of several contaminants in landfill leachate can cause a series of mechanisms in adsorption which can occur in the solute system.

However, in general, the first adsorption layer forms due to the binding of the surface functional groups of the adsorbent with molecules/ions of the adsorbate. The subsequent adsorption layers are created on the surface of the adsorbent according to the geometry of the adsorbate (Sharififard, 2018).

Biosorbents such as chitosan, are rich in nitrogen in the form of amino groups, and oxygen in the hydroxyl groups which exist in their molecule chain (Wang and Zhuang, 2017). These can bind anionic contaminants with the contribution of the mechanisms of hydrogen bonding, ion-exchange adsorption and molecular interactions induced by Van Der Waals forces. Protonation of the amine groups as observed by FTIR spectra, further affirms the existence of electrostatic attractions with anions leading to enhanced anion uptake (Sirajudheen et al., 2021; Vakili et al., 2018). Electrostatic attraction occurs between CHT-CLP and water because of the replacement of hydrogen bonds by anionic contaminants due to comparatively higher affinity (Shajahana et al., 2017). In addition, achieving a comparatively effective regeneration when using distilled water as the eluting agent gives evidence that the adsorption may have been caused by weak physical bonding of the colour-causing molecules with the adsorbent surface (Santra et al., 2020).

Metal cations can be interacted with the non-bonded electron pair of nitrogen on amine groups at neutral and acidic pH due to the influence of H^+ on NH_2 groups and hence will be more prone to attract metal cations creating complexes (Guibal, 2004; Nagireddi et al., 2017).

Table 5
ANOVA Results for the quadratic model for Colour Removal using CHT-CLP.

Source	Sum of Squares	df	Mean Square	F-value	p-value
Model	9584.72	9	1064.97	83,246.77	<0.0001
A-pH	792.42	1	792.42	61,941.93	<0.0001
B-Adsorbent Dosage	3479.45	1	3479.45	2.720E+05	<0.0001
C-Contact Time	230.70	1	230.70	18,033.04	<0.0001
AB	16.62	1	16.62	1298.97	<0.0001
AC	331.68	1	331.68	25,927.09	<0.0001
BC	54.67	1	54.67	4273.56	<0.0001
A^2	882.55	1	882.55	68,987.16	<0.0001
B^2	1490.09	1	1490.09	1.165E+05	<0.0001
C^2	151.00	1	151.00	11,803.30	<0.0001
Residual	0.0384	3	0.0128		
Lack of Fit	0.0384	1	0.0384		
Pure Error	0.0000	2	0.0000		
Cor Total	9584.76	12			

In addition, as observed in the SEM images and according to BET-SSA analysis, the development of the porous structure and surface area of the material with holes and small openings on the surface further facilitates pore filling and pore diffusion during adsorption. Furthermore, pH_{ZPC} being 4.8 (< pH 7) further assists the penetration of the contaminants inside the pores favouring the anion uptake.

3.6. Optimization of colour removal by CHT-CLP using RSM

The optimization of CHT-CLP was evaluated on the colour removal percentage.

The experimental design obtained and their respective responses in each experimental run are provided in supplementary materials [Table S1]. The contributions of the operational and interaction factors that influenced the colour removal were evaluated using ANOVA which are tabulated in Table 5. The effectiveness of the model was evaluated based on the coefficient of determination (Galan et al., 2021). R^2 and Adj R^2 which showed a value of 1.00 indicates a very good correlation between the input and output variables. It was also noted that the larger

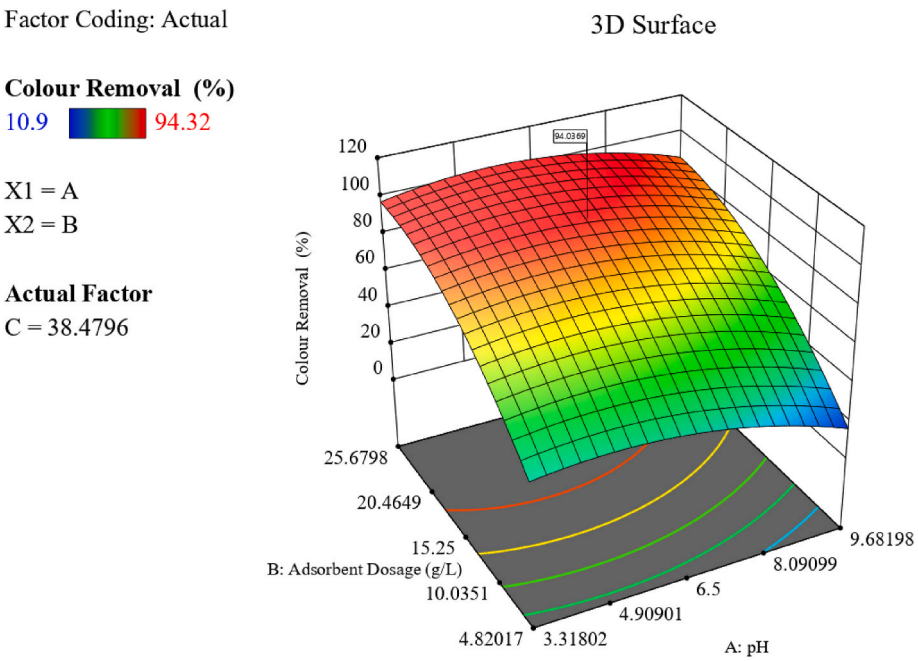

Fig. 8. 3D Surface obtained for optimized solution for colour removal. (For interpretation of the references to colour in this figure legend, the reader is referred to the Web version of this article.)

F-value and p-value <0.05, indicated that the model is significant (Pambi and Musonge, 2016). Adequate precision (840.9) indicated an adequate signal suggesting that this model can be used to navigate the design space. Similarly, based on the experimental data, the coded quadratic model equation was established as equation (1).

$$Colour\ Removal\ (\%) = 82.34 - 14.07A + 29.49B + 7.59C + 2.67AB + 11.59AC + 5.58BC - 10.70A^2 - 14.84B^2 - 4.68C^2 \quad (1)$$

where A is the pH of the solution, B is the adsorbent dosage of CHT-CLP (g) and C is the contact time (h).

Fig. 8 shows that the optimum conditions can achieve a colour removal of 94.04%. As observed in batch experiments, increasing the pH and reducing the adsorbent dosage have negatively affected the colour removal which validates the predictions given by the model.

Hence, equation (1) can be used for predicting the colour removal efficiency by CHT-CLP when integrated with a biological treatment system. The effectiveness of the material for different types of wastewater can be assessed by substituting the respective wastewater conditions to obtain the predicted removal efficiency. This will be beneficial as it indicates if CHT-CLP would be a viable material for the considered system, before implementing it practically in a treatment sequence. This method also gives the benefit of expanding the material range and can be studied in less amount of time to create a database for adsorptive efficiencies of materials which can ultimately be used worldwide for a range of wastewater types.

4. Conclusions

This study investigated the versatility of crosslinked protonated chitosan as a biosorbent for colour removal as a post-treatment for landfill leachate. Adsorbent dosage, pH and contact time played major roles on the removal efficiency marking their optimum values at 20 g/L, 2 and 48 h respectively to achieve a removal efficiency of 96 ± 3.8%. These observations suggest that CHT-CLP can significantly adsorb colour from aqueous solutions at acidic pH levels even though raw chitosan beads tend to dissolve at low pH conditions. The adsorption process was satisfactorily described by Pseudo-Second-Order kinetics and equilibrium data fitted well with the Langmuir isotherm model with a monolayer adsorption capacity of 123.8 Pt–Co/g. Adsorption and regeneration capacities demonstrated by CHT-CLP prove that it is an effective, potential biosorbent that can be applied for the colour removal from biologically pre-treated landfill leachate, to reach the discharge limits of the Central Environmental Authority of Sri Lanka. The statistical analysis proved that the application of RSM could generate model equations that are useful in predicting and optimizing the colour removal process.

Author contributions

W.S.M.S.K. Wijerathna: Conceptualization, Data Curation, Methodology, Software, Validation, Formal Analysis, Investigation, Writing – Original Draft. **L.M.L.K.B. Lindamulla:** Methodology **K.G.N. Nanayakkara:** Conceptualization, Methodology, Resources, Writing – Review & Editing, Supervision, Funding acquisition. **R.M.L.D. Rathnayake:** Resources, Writing – Review & Editing, Supervision. **V. Jegatheesan:** Writing – Review & Editing, Supervision. **K.B.S.N. Jinadasa:** Resources, Supervision.

Declaration of competing interest

The authors declare that they have no known competing financial interests or personal relationships that could have appeared to influence the work reported in this paper.

Data availability

Data will be made available on request.

Acknowledgements

Authors gratefully acknowledge the scholarship provided by the Postgraduate Programme in Civil Engineering, University of Peradeniya, Sri Lanka to the first author and the chitosan material received from the Norwegian University of Life Sciences.

Appendix A. Supplementary data

Supplementary data to this article can be found online at https://doi.org/10.1016/j.envres.2022.115018.

References

Abuabdou, S.M.A., Teng, O.W., Bashir, M.J.K., Aun, N.C., Sethupathi, S., Pratt, L.M., 2019. Treatment of tropical stabilised landfill leachate using palm oil fuel ashisothermal and kinetic studies. Desalination Water Treat. 144, 201–210. https://doi.org/10.5004/dwt.2019.23662.

Adeleke, A.O., Latiff, A.A.A., Al-Gheethi, A.A., Daud, Z., 2017. Optimization of operating parameters of novel composite adsorbent for organic pollutants removal from POME using response surface methodology. Chemosphere 174, 232–242. https://doi.org/10.1016/j.chemosphere.2017.01.110.

Alves, D.C. da S., Healy, B., Pinto, L.A.d.A., Cadaval, T.R.S., Breslin, C.B., 2021. Recent developments in Chitosan-based adsorbents for the removal of pollutants from aqueous environments. Molecules 26. https://doi.org/10.3390/molecules26030594.

APHA, 2002. American public health association; American water works association; water environment federation. Stand. Methods Exam. Water Wastewater 2, 1–541.

Azis, K., Mavriou, Z., Karpouzas, D.G., Ntougias, S., Melidis, P., 2021. Evaluation of sand filtration and activated carbon adsorption for the post-treatment of a secondary biologically-treated fungicide-containing wastewater from fruit-packing industries. Processes 9, 1223.

Aziz, H.A., Foul, A.A., Isa, M.H., Hung, Y.T., 2010. Physico-chemical treatment of anaerobic landfill leachate using activated carbon and zeolite: batch and column studies. Int. J. Environ. Waste Manag. 5, 269–285. https://doi.org/10.1504/IJEWM.2010.032008.

Aziz, H.A., Hin, L.T., Adlan, M.N., Zahari, M.S., Alias, S., Ahmed, A.M., Selamat, M.R., Bashir, M.J.K., Yusoff, M.S., Umar, M., 2011. Removal of high-strength colour from semi-aerobic stabilized landfill leachate via adsorption on limestone and activated carbon mixture. Res. J. Chem. Sci. 1, 1–7.

Aziz, H.A., Noor, A.F.M., Keat, Y.W., Alazaiza, M.Y.D., Hamid, A.A., 2020. Heat activated Zeolite for the reduction of ammoniacal nitrogen, colour, and COD in landfill leachate. Int. J. Environ. Res. 14, 463–478. https://doi.org/10.1007/s41742-020-00270-5.

Azmi, N.B., Bashir, M.J.K., Sethupathi, S., Wei, L.J., Aun, N.C., 2014. Stabilized landfill leachate treatment by sugarcane bagasse derived activated carbon for removal of color, COD and NH3-N - optimization of preparation conditions by RSM. J. Environ. Chem. Eng. 3, 1287–1294. https://doi.org/10.1016/j.jece.2014.12.002.

Bakatula, E.N., Richard, D., Neculita, C.M., Zagury, G.J., 2018. Determination of point of zero charge of natural organic materials. Environ. Sci. Pollut. Res. 25, 7823–7833. https://doi.org/10.1007/s11356-017-1115-7.

Bodzek, M., Łobos-Moysa, E., Zamorowska, M., 2006. Removal of organic compounds from municipal landfill leachate in a membrane bioreactor. Desalination 198, 16–23. https://doi.org/10.1016/j.desal.2006.09.004.

Bui, T.H., Lee, W., Jeon, S.B., Kim, K.W., Lee, Y., 2020. Enhanced Gold(III) adsorption using glutaraldehyde-crosslinked chitosan beads: effect of crosslinking degree on adsorption selectivity, capacity, and mechanism. Separ. Purif. Technol. 248, 116989 https://doi.org/10.1016/j.seppur.2020.116989.

Castillo-Suárez, L.A., Bruno-Severo, F., Lugo-Lugo, V., Esparza-Soto, M., Martínez-Miranda, V., Linares-Hernández, I., 2018. Peroxicoagulation and solar peroxicoagulation for landfill leachate treatment using a Cu–Fe system. Water, Air, Soil Pollut. 229 https://doi.org/10.1007/s11270-018-4031-7.

Castrillón, L., Fernández-Nava, Y., Ulmanu, M., Anger, I., Marañón, E., 2010. Physico-chemical and biological treatment of MSW landfill leachate. Waste Manag. 30, 228–235. https://doi.org/10.1016/j.wasman.2009.09.013.

CEA, 2008. National Environmental (Protection and Quality) Regulations, No. 1 of 2008, the Gazette of the Democratic Socialist Republic of Sri Lanka.

Chaouki, Z., El Mrabet, I., Khalil, F., Ijjaali, M., Rafqah, S., Anouar, S., Nawdali, M., Valdés, H., Zaitan, H., 2017. Use of coagulation-flocculation process for the treatment of the landfill leachates of Casablanca city (Morocco). J. Mater. Environ. Sci. 8, 2781–2791.

Chaouki, Z., Hadri, M., Nawdali, M., Benzina, M., Zaitan, H., 2021. Treatment of a landfill leachate from Casablanca city by a coagulation-flocculation and adsorption process using a palm bark powder (PBP). Sci. African 12, e00721. https://doi.org/10.1016/j.sciaf.2021.e00721.

Choi, H.Y., Bae, J.H., Hasegawa, Y., An, S., Kim, I.S., Lee, H., Kim, M., 2020. Thiol-functionalized cellulose nanofiber membranes for the effective adsorption of heavy metal ions in water. Carbohydr. Polym. 234, 115881 https://doi.org/10.1016/j.carbpol.2020.115881.

Costa, A.M., , Alfaia, R.G. de S.M., Campos, J.C., 2019. Landfill leachate treatment in Brazil – an overview. J. Environ. Manag. 232, 110–116. https://doi.org/10.1016/j.jenvman.2018.11.006.

De, S., Hazra, T., Dutta, A., 2019. Treatment of landfill leachate by integrated sequence of air stripping, coagulation–flocculation and adsorption. Environ. Dev. Sustain. 21, 657–677. https://doi.org/10.1007/s10668-017-0053-3.

Fenyvesi, É., Barkács, K., Gruiz, K., Varga, E., Kenyeres, I., Záray, G., Szente, L., 2020. Removal of hazardous micropollutants from treated wastewater using cyclodextrin bead polymer – a pilot demonstration case. J. Hazard Mater. 383, 121181 https://doi.org/10.1016/j.jhazmat.2019.121181.

Ferraz, F.M., Yuan, Q., 2020. Performance of oat hulls activated carbon for COD and color removal from landfill leachate. J. Water Proc. Eng. 33, 101040 https://doi.org/10.1016/j.jwpe.2019.101040.

Filipkowska, U., Jóźwiak, T., Szymczyk, P., 2014. Application of cross-linked chitosan for phosphate removal from aqueous solutions. Prog. Chem. Appl. Chitin its Deriv. 19, 5–14. https://doi.org/10.15259/PCACD.19.01.

Foo, K.Y., Hameed, B.H., 2010. Insights into the modeling of adsorption isotherm systems. Chem. Eng. J. 156, 2–10. https://doi.org/10.1016/j.cej.2009.09.013.

Foo, K.Y., Hameed, B.H., 2009. An overview of landfill leachate treatment via activated carbon adsorption process. J. Hazard Mater. 171, 54–60. https://doi.org/10.1016/j.jhazmat.2009.06.038.

Foo, K.Y., Lee, L.K., Hameed, B.H., 2013a. Preparation of tamarind fruit seed activated carbon by microwave heating for the adsorptive treatment of landfill leachate: a laboratory column evaluation. Bioresour. Technol. 133, 599–605. https://doi.org/10.1016/j.biortech.2013.01.097.

Foo, K.Y., Lee, L.K., Hameed, B.H., 2013b. Batch adsorption of semi-aerobic landfill leachate by granular activated carbon prepared by microwave heating. Chem. Eng. J. 222, 259–264. https://doi.org/10.1016/j.cej.2013.02.032.

Foul, A.A., Aziz, H.A., Isa, M.H., Hung, Y.-T., 2009. Primary treatment of anaerobic landfill leachate using activated carbon and limestone : batch and column studies. Int. J. Environ. Waste Manag. 4, 282–298.

Galan, J., Trilleras, J., Zapata, P.A., Arana, V.A., Grande-Tovar, C.D., 2021. Optimization of chitosan glutaraldehyde-crosslinked beads for reactive blue 4 anionic dye removal using a surface response methodology. Life 11, 1–20. https://doi.org/10.3390/life11020085.

Ghani, Z.A., Yusoff, M.S., Zaman, N.Q., Zamri, M.F.M.A., Andas, J., 2017. Optimization of preparation conditions for activated carbon from banana pseudo-stem using response surface methodology on removal of color and COD from landfill leachate. Waste Manag. 62, 177–187. https://doi.org/10.1016/j.wasman.2017.02.026.

Guibal, E., 2004. Interactions of metal ions with chitosan-based sorbents: a review. Separ. Purif. Technol. 38, 43–74. https://doi.org/10.1016/j.seppur.2003.10.004.

Guibal, E., Milot, C., Tobin, J.M., 1998. Metal-anion sorption by chitosan beads: equilibrium and kinetic studies. Ind. Eng. Chem. Res. 37, 1454–1463. https://doi.org/10.1021/ie9703954.

Hagemann, N., Schmidt, H.P., Kägi, R., Böhler, M., Sigmund, G., Maccagnan, A., McArdell, C.S., Bucheli, T.D., 2020. Wood-based activated biochar to eliminate organic micropollutants from biologically treated wastewater. Sci. Total Environ. 730, 138417 https://doi.org/10.1016/j.scitotenv.2020.138417.

Halim, N.H.M., Adnan, R., Lahuri, A.H., Jaafar, N.F., Nordin, N., 2022. Exploring the potential of highly efficient graphite/chitosan–PVC composite electrodes in the electrochemical degradation of Reactive Red 4. J. Chem. Technol. Biotechnol. 97, 147–159. https://doi.org/10.1002/jctb.6924.

Huang, R., Yang, B., Liu, Q., Ding, K., 2012. Removal of fluoride ions from aqueous solutions using protonated cross-linked chitosan particles. J. Fluor. Chem. 141, 29–34. https://doi.org/10.1016/j.jfluchem.2012.05.022.

Huang, X.Y., Bu, H.T., Jiang, G.B., Zeng, M.H., 2011. Cross-linked succinyl chitosan as an adsorbent for the removal of Methylene Blue from aqueous solution. Int. J. Biol. Macromol. 49, 643–651. https://doi.org/10.1016/j.ijbiomac.2011.06.023.

Hussain, S., Kamran, M., Khan, S.A., Shaheen, K., Shah, Z., Suo, H., Khan, Q., Shah, A.B., Rehman, W.U., Al-Ghamdi, Y.O., Ghani, U., 2021. Adsorption, kinetics and thermodynamics studies of methyl orange dye sequestration through chitosan composites films. Int. J. Biol. Macromol. 168, 383–394. https://doi.org/10.1016/j.ijbiomac.2020.12.054.

Igberase, E., Osifo, P., Ofomaja, A., 2017. The adsorption of Pb, Zn, Cu, Ni, and Cd by modified ligand in a single component aqueous solution: equilibrium, kinetic, thermodynamic, and desorption studies. Int. J. Anal. Chem. 2017. https://doi.org/10.1155/2017/6150209.

Jawad, A.H., Mubarak, N.S.A., Abdulhameed, A.S., 2019. Tunable Schiff's base-cross-linked chitosan composite for the removal of reactive red 120 dye: adsorption and mechanism study. Int. J. Biol. Macromol. https://doi.org/10.1016/j.ijbiomac.2019.10.014.

Jiang, B., Wang, J., Chen, L., Sun, Y., Wang, X., Ruan, J., 2022. Experimental study on the treatment of landfill leachate by electro-assisted ZVI/UV synergistic activated persulfate system. Catalysts 12. https://doi.org/10.3390/catal12070768.

Koliyabandara, S.M.P.A., Asitha, T.C., Sudantha, L., Siriwardana, C., 2020. Assessment of the impact of an open dumpsite on the surface water quality deterioration in Karadiyana, Sri Lanka. Environ. Nanotechnol. Monit. Manag. 14, 100371 https://doi.org/10.1016/j.enmm.2020.100371.

Lebron, Y.A.R., Moreira, V.R., Brasil, Y.L., Silva, A.F.R., Santos, L.V. de S., Lange, L.C., Amaral, M.C.S., 2021. A survey on experiences in leachate treatment: common practices, differences worldwide and future perspectives. J. Environ. Manag. 288 https://doi.org/10.1016/j.jenvman.2021.112475.

Lindamulla, L.M.L.K.B., Jayawardene, N.K.R.N., Wijerathne, W.S.M.S.K., Othman, M., Nanayakkara, K.G.N., Jinadasa, K.B.S.N., Herath, G.B.B., Jegatheesan, V., 2022. Treatment of mature landfill leachate in tropical climate using membrane bioreactors with different configurations. Chemosphere 307, 136013. https://doi.org/10.1016/j.chemosphere.2022.136013.

Liu, Q., Hu, P., Wang, J., Zhang, L., Huang, R., 2016. Phosphate adsorption from aqueous solutions by Zirconium (IV) loaded cross-linked chitosan particles. J. Taiwan Inst. Chem. Eng. 59, 311–319. https://doi.org/10.1016/j.jtice.2015.08.012.

Luo, H., Zeng, Y., Cheng, Y., He, D., Pan, X., 2019. Recent advances in municipal landfill leachate: a review focusing on its characteristics, treatment, and toxicity assessment. Sci. Total Environ. https://doi.org/10.1016/j.scitotenv.2019.135468.

Mahaninia, M.H., Wilson, L.D., 2017. A kinetic uptake study of roxarsone using cross-linked chitosan beads. Ind. Eng. Chem. Res. 56, 1704–1712. https://doi.org/10.1021/acs.iecr.6b04412.

Marañón, E., Castrillón, L., Fernández-Nava, Y., Fernández-Méndez, A., Fernández-Sánchez, A., 2009. Tertiary treatment of landfill leachates by adsorption. Waste Manag. Res. 27, 527–533. https://doi.org/10.1177/0734242X08096900.

Nagireddi, S., Katiyar, V., Uppaluri, R., 2017. Pd (II) adsorption characteristics of glutaraldehyde cross-linked chitosan copolymer resin. Int. J. Biol. Macromol. 94, 72–84.
Narayana, S.K.V., 2022. Kaolinite-chitosan based nano-composites and applications. In: Adv. App. Of Micro and Nano Clay – Biopolymer-Based Composites, pp. 87–102.
Nassar, M.M., El-Geundi, M.S., 1991. Comparative cost of colour removal from textile effluents using natural adsorbents. J. Chem. Technol. Biotechnol. 50, 257–264. https://doi.org/10.1002/jctb.280500210.
Ngah, W.S.W., Ab Ghani, S., Kamari, A., 2005. Adsorption behaviour of Fe(II) and Fe(III) ions in aqueous solution on chitosan and cross-linked chitosan beads. Bioresour. Technol. 96, 443–450. https://doi.org/10.1016/j.biortech.2004.05.022.
Ngah, W.S.W., Fatinathan, S., 2008. Adsorption of Cu(II) ions in aqueous solution using chitosan beads, chitosan-GLA beads and chitosan-alginate beads. Chem. Eng. J. 143, 62–72. https://doi.org/10.1016/j.cej.2007.12.006.
Pambi, R.L.L., Musonge, P., 2016. Application of response surface methodology (RSM) in the treatment of final effluent from the sugar industry using Chitosan. Water Pollut. XIII 1, 209–219. https://doi.org/10.2495/wp160191.
Pratiwi, R.A., Nandiyanto, A.B.D., 2022. How to read and interpret UV-VIS spectrophotometric results in determining the structure of chemical compounds. Indones. J. Educ. Res. Technol. 2, 1–20. https://doi.org/10.17509/ijert.v2i1.35171.
Ravikumar, K., Krishnan, S., Ramalingam, S., Balu, K., 2007. Optimization of process variables by the application of response surface methodology for dye removal using a novel adsorbent. Dyes Pigments 72, 66–74. https://doi.org/10.1016/j.dyepig.2005.07.018.
Ribera-Pi, J., Badia-Fabregat, M., Espí, J., Clarens, F., Jubany, I., Martínez-Lladó, X., 2021. Decreasing environmental impact of landfill leachate treatment by MBR, RO and EDR hybrid treatment. Environ. Technol. 42, 3508–3522. https://doi.org/10.1080/09593330.2020.1734099.
Rosli, M.A., Daud, Z., Awang, H., Ab Aziz, N.A., Ridzuan, M.B., Abubakar, M.H., Adnan, M.S., Tajarudin, H.A., 2018. Adsorption efficiency and isotherms of COD and color using Limestone and zeolite adsorbents. Int. J. Integr. Eng. 10, 8–13. https://doi.org/10.30880/ijie.2018.10.08.011.
Rosli, M.A., Daud, Z., Latiff, A.A.A., Rahman, S.E.A., Oyekanmi, A.A., Zainorabidin, A., Awang, H., Halim, A.A., 2017. The effectiveness of Peat-AC composite adsorbent in removing color and Fe from landfill leachate. Int. J. Integr. Eng. 9, 35–38.
Rupasinghe, N.K.L.C., Senanayake, S.M.A.E., Nanayakkara, K.G.N., 2022. Development, characterization and mechanisms study of protonated sawdust biochar-chitosan composite bead biosorbent for defluoridation of contaminated groundwater. Bioresour. Technol. Reports 17. https://doi.org/10.1016/j.biteb.2022.100946.
San-Pedro, L., Méndez-Novelo, R., Hernández-Núñez, E., Flota-Bañuelos, M., Medina, J., Giacomán-Vallejos, G., 2020. Selection of the activated carbon type for the treatment of landfill leachate by fenton-adsorption process. Molecules 25. https://doi.org/10.3390/molecules25133023.
Sánchez-Duarte, R.G., Sánchez-Machado, D.I., López-Cervantes, J., Correa-Murrieta, M. A., 2012. Adsorption of allura red dye by cross-linked chitosan from shrimp waste. Water Sci. Technol. 65, 618–623. https://doi.org/10.2166/wst.2012.900.
Santra, B., Ramrakhiani, L., Kar, S., Ghosh, S., Majumdar, S., 2020. Ceramic membrane-based ultrafiltration combined with adsorption by waste derived biochar for textile effluent treatment and management of spent biochar. J. Environ. Heal. Sci. Eng. 18, 973–992. https://doi.org/10.1007/s40201-020-00520-w.
Shajahana, A., Shankar, S., Sathiyaseelan, A., Narayan, K.S., Narayanan, V., Kaviyarasan, V., Ignacimuthu, S., 2017. Comparative studies of chitosan and its nanoparticles for the adsorption efficiency of various dyes. Int. J. Biol. Macromol. 104, 1449–1458.
Sharififard, H., 2018. Statistical physics modeling of equilibrium adsorption of cadmium ions onto activated carbon, chitosan and chitosan/activated carbon composite. Adv. Environ. Sci. Technol. 4, 149–154. https://doi.org/10.22104/aet.2019.2619.1132.
Shukla, S.K., Pandey, S., Saha, S., Singh, H.R., Mishra, P.K., Kumar, S., Jha, S.K., 2021. Removal of crystal violet by Cu-chitosan nano-biocomposite particles using Box–Behnken design. J. Environ. Chem. Eng. 9, 105847 https://doi.org/10.1016/j.jece.2021.105847.
Sirajudheen, P., Poovathumkuzhi, N.C., Vigneshwaran, S., Chelaveettil, B.M., Meenakshi, S., 2021. Applications of chitin and chitosan based biomaterials for the adsorptive removal of textile dyes from water — a comprehensive review. Carbohydr. Polym. 273, 118604 https://doi.org/10.1016/j.carbpol.2021.118604.
Sivakami, M.S., Gomathi, T., Venkatesan, J., Jeong, H.S., Kim, S.K., Sudha, P.N., 2013. Preparation and characterization of nano chitosan for treatment wastewaters. Int. J. Biol. Macromol. 57, 204–212. https://doi.org/10.1016/j.ijbiomac.2013.03.005.
Sowmya, A., Meenakshi, S., 2014. Zr(IV) loaded cross-linked chitosan beads with enhanced surface area for the removal of nitrate and phosphate. Int. J. Biol. Macromol. 69, 336–343. https://doi.org/10.1016/j.ijbiomac.2014.05.043.
Suguna, M., Siva Kumar, N., Subba Reddy, A., Boddu, V.M., Krishnaiah, A., 2011. Biosorption of lead(II) from aqueous solution on glutaraldehyde cross-linked chitosan beads. Can. J. Chem. Eng. 89, 833–843. https://doi.org/10.1002/cjce.20462.
Sun, S., Wang, L., Wang, A., 2006. Adsorption properties of crosslinked carboxymethyl-chitosan resin with Pb(II) as template ions. J. Hazard Mater. 136, 930–937. https://doi.org/10.1016/j.jhazmat.2006.01.033.
Tabrizi, N.S., Yavari, M., 2020. Fixed bed study of nitrate removal from water by protonated cross-linked chitosan supported by biomass-derived carbon particles. J. Environ. Sci. Heal. - Part A Toxic/Hazardous Subst. Environ. Eng. 55, 777–787. https://doi.org/10.1080/10934529.2020.1741998.
Tahari, N., de Hoyos-Martinez, P.L., Izaguirre, N., Houwaida, N., Abderrabba, M., Ayadi, S., Labidi, J., 2022. Preparation of chitosan/tannin and montmorillonite films as adsorbents for Methyl Orange dye removal. Int. J. Biol. Macromol. 210, 94–106. https://doi.org/10.1016/j.ijbiomac.2022.04.231.
Thongkrua, S., Suriya, P., 2022. Removal of colour and COD in biologically pre-treated leachate using activated carbon from corn cobs. Pollution 8, 657–670. https://doi.org/10.22059/POLL.2022.328345.1153.
Vaccari, M., Tudor, T., Vinti, G., 2019. Characteristics of leachate from landfills and dumpsites in Asia, Africa and Latin America: an overview. Waste Manag. 95, 416–431. https://doi.org/10.1016/j.wasman.2019.06.032.
Vakili, M., Deng, S., Li, T., Wang, Wei, Wang, Wenjing, Yu, G., 2018. Novel crosslinked chitosan for enhanced adsorption of hexavalent chromium in acidic solution. Chem. Eng. J. 347, 782–790. https://doi.org/10.1016/j.cej.2018.04.181.
Vakili, M., Mojiri, A., Zwain, H.M., Yuan, J., Giwa, A.S., Wang, W., Gholami, F., Guo, X., Cagnetta, G., Yu, G., 2019. Effect of beading parameters on cross-linked chitosan adsorptive properties. React. Funct. Polym. 144, 104354 https://doi.org/10.1016/j.reactfunctpolym.2019.104354.
Vedula, S.S., Yadav, G.D., 2022. Wastewater treatment containing methylene blue dye as pollutant using adsorption by chitosan lignin membrane: development of membrane, characterization and kinetics of adsorption. J. Indian Chem. Soc. 99, 100263 https://doi.org/10.1016/j.jics.2021.100263.
Vieira, R.S., Oliveira, M.L.M., Guibal, E., Rodríguez-Castellón, E., Beppu, M.M., 2011. Copper, mercury and chromium adsorption on natural and crosslinked chitosan films: an XPS investigation of mechanism. Colloids Surfaces A Physicochem. Eng. Asp. 374, 108–114. https://doi.org/10.1016/j.colsurfa.2010.11.022.
Vogelsang, C., Andersen, D.O., Hey, A., Hakonsen, T., Jantsch, T.G., Müller, E.D., Pedersen, M.A., Varum, K.M., 2004. Removal of humic substances by chitosan. Water Sci. Technol. Water Supply 4, 121–129. https://doi.org/10.2166/ws.2004.0100.
Wang, J., Guo, X., 2020a. Adsorption kinetic models: physical meanings, applications, and solving methods. J. Hazard Mater. 390, 122156 https://doi.org/10.1016/j.jhazmat.2020.122156.
Wang, J., Guo, X., 2020b. Adsorption isotherm models: classification, physical meaning, application and solving method. Chemosphere 258, 127279. https://doi.org/10.1016/j.chemosphere.2020.127279.
Wang, J., Zhuang, S., 2017. Removal of various pollutants from water and wastewater by modified chitosan adsorbents. Crit. Rev. Environ. Sci. Technol. 47, 2331–2386. https://doi.org/10.1080/10643389.2017.1421845.
Wijesekara, S.S.R.M.D.H.R., Mayakaduwa, S.S., Siriwardana, A.R., de Silva, N., Basnayake, B.F.A., Kawamoto, K., Vithanage, M., 2014. Fate and transport of pollutants through a municipal solid waste landfill leachate in Sri Lanka. Environ. Earth Sci. 72, 1707–1719. https://doi.org/10.1007/s12665-014-3075-2.
Zafar, S., Khan, M.I., Lashari, M.H., Khraisheh, M., Almomani, F., Mirza, M.L., Khalid, N., 2020. Removal of copper ions from aqueous solution using NaOH-treated rice husk. Emergent Mater 3, 857–870. https://doi.org/10.1007/s42247-020-00126-w.